Int J Clin Exp Pathol 2019;12(9):3583-3594
www.ijcep.com /ISSN:1936-2625/IJCEP0093722

Original Article

Characterization of TCF4-mediated oncogenic role in cutaneous squamous cell carcinoma

Yun Li[1], Chunling Huang[2], Xichuan Yang[1]

[1]Department of Dermatology, The First Affiliated Hospital of The Army Medical University, Chongqing 400038, P.R. China; [2]Laboratory of Reproductive Biology, School of Public Health and Management, Chongqing Medical University, Chongqing 400038, P.R. China

Received March 12, 2019; Accepted June 24, 2019; Epub September 1, 2019; Published September 15, 2019

Abstract: The aberrant highly expressed T-cell factor 4 (TCF4) has been determined to be closely connected with carcinogenesis of cutaneous squamous cell carcinoma (cSCC) in previous studies. However, the underlying regulatory network and the potential therapeutic targets of TCF4 in SCC are still not fully understood. In this study, the highly expressed TCF4 was observed in human cSCC cancer compared to the paired adjacent tissues. A431 cell lines with TCF4 RNA silencing were found to be the repressive cell proliferation and invasion as well as the enhanced apoptosis. Furthermore, RNA-Seq was conducted and observed that 147 genes were up-regulated (including 113 coding genes and 34 lncRNA) while 172 genes were down-regulated (including 64 coding genes and 108 lncRNA) in TCF4 silencing compared to blank RNAi and untreated control A431 cells. 18 pathways including steroid, porphyrin, arachidonic acid, and retinol metabolism, as well as the functions associated with angiogenesis, inflammatory response, and cell adhesion were involved in the differentially expressed genes of A431 cells with TCF4 silencing. Finally, ChIP-qPCR of TCF4 and β-catenin were performed and we found that the enrichments of β-catenin were lost on the promoters on top ten down-regulated genes in A431 cells with TCF4 silencing compared to the untreated A431. Additionally, in untreated A431 cells, some genes such as ALDH8A1, DRICH1, and UGT1A5 were observed with high enrichment of TCF4, but without β-catenin, which indicated a Wnt/β-catenin independent way of TCF4 for gene transcriptional regulation. In conclusion, we declared that TCF4 played an important role in tumorigenesis of skin cancer via the aberrant activation of variety of signaling pathways, and could be considered as a potential therapeutic target for cSCC treatment.

Keywords: TCF4, Wnt/β-catenin, cutaneous squamous cell carcinoma, RNA-Seq

Introduction

Skin cancers are arisen from the uncontrolled growth of abnormal skin cells which primarily developed on the exposure to ultraviolet (UV) radiation from sunlight or tanning beds. Skin cancers are classified as basal cell carcinoma, cutaneous squamous cell carcinoma (cSCC), and melanoma. Epidemiologic studies have declared that cSCC accounts for 20% of total skin cancer with the continuously increasing incidence worldwide and poses a threat for public health [1, 2]. A significant subset of cSCC has the propensity for poor outcomes [3]. Besides the cause of UV exposure, the genetic reasons, especially the disabled DNA damage repair for UV, induced cyclobutene pyrimidine dimers contribute to the cSCC development [4]. Moreover, the regulatory network for cell growth, apoptosis, and invasion had also attracted the attention in carcinogenesis of cSCC.

T-cell factor 4 (TCF4) is a high mobility group (HMG) box-containing transcription factor, which is broadly expressed in various tissues. Furthermore, TCF4 has been determined to activate Wnt/β-catenin signaling pathway in multiple cancers including colon cancer, hepatocellular carcinoma, and osteosarcoma [5-7]. Silencing the aberrant expression of TCF4 can efficiently repress the tumor cell growth and proliferation, which indicates that TCF4 plays an oncogenic role and can be served as a potential therapeutic target for cancer treatment.

Table 1. The clinical information of the patients are listed

Serial number	Age (year)	Gender	Stage
cSSC_1	51	F	III
cSSC_2	48	F	IV
cSSC_3	61	M	IV
cSSC_4	69	F	III
cSSC_5	41	M	III
cSSC_6	64	F	IV
cSSC_7	54	F	IV
cSSC_8	58	M	III
cSSC_9	62	M	IV
cSSC_10	49	M	III

However, the roles and the underlying mechanism of TCF4 in the carcinogenesis and development of cSCC are not fully understood.

In this study, we blocked TCF4 in A431 cSCC cell lines using RNAi, and investigated the effect of morphology and transcriptome of skin cancer cells. Besides the Wnt/β-catenin signaling pathway, we also observed that other regulatory pathways also changed upon TCF4 knockdown. Our study attempted to illustrate the crucial role of TCF in the focus of the regulatory mechanism underlying signaling pathway and network in cSCC and provided the potential therapeutic targets for cSCC treatment.

Materials and methods

Clinical samples

Ten paired cSCC and adjacent normal tissues were collected by the First Affiliated Hospital of the Army Medical University from 2015-2017. The clinical information of the patients was listed in **Table 1**. Signed informed consent and ethics committee documents of Ethics Committee of The First Affiliated Hospital of the Army Medical University were all provided to approve this study.

Immunohistochemistry

5 μm paraffin tissue sections were taken and dewaxed by hydration and immediately put into 3% H_2O_2 methanol to remove endogenous catalase. After incubation for 10 min, antigens were retrieved. After that, sections were added to the citric acid buffer, boiled for 2 min, and naturally cooled at room temperature. Following, drops of 5% BSA blocking solution was added and placed at room temperature for 30 min in terms of which drops of TCF4 antibody were added and stored at 4°C overnight. After restoration to room temperature, the secondary anti-goat antibody and S-P reagent was added and the mixture was washed thrice with PBS. After DAB coloration, counterstain, dehydration until transparency, and timely mounting, microscopic examination was performed. The positive staining was statistically analyzed using Image J.

Cell culture

cSCC A431 cell lines (ATCC, USA) were cultured within Dulbecco's Modified Eagle Medium (DMEM) with 1.5 mM L-Glutamine and 10% Fetal Bovine Serum (FBS) (Thermo Fisher Scientific, USA) in an incubator of 37°C, 5% CO_2 and appropriate humidity. Three TCF4 siRNA oligo (siRNA_1: 5'-GGAGUUGGUUCUGUAUUAUUU-3', siRNA_2: 5'-CCGGGAAAGUUUGGAAGAA-3', siRNA_3: GACCCAUUCUUAUUUCAAUUU-3') was (GenePharma, China) transfected into A431 cells by lipofectamine 2000 (Thermo Fisher Scientific, USA) to validate the effectiveness. The siRNA (Sense: 5'-UUCUCCGAACGUGUCACGUTT-3', Antisense: 5'-ACGUGACACGUUCGGAGAATT-3') with no significant sequence similarity to human gene sequence was also treated as a blank control. Non-treated A431 cell was used as a negative control.

Methylthiazoletetrazolium (MTT) assay

Cells were passaged into 96-well plates with a density of 1 × 10^5 cells/well, and treated with a gradient concentration of 0.2, 0.4, 0.8, and 1.6 mg/ml MTT (Sinopharm Chemical Reagent, China) for 6 hour incubation. Then, they were washed by PBS twice, and incubated for 10 minutes with 200 μl DMSO in the dark, followed by detection of the absorbance value at 570 nm by a microplate reader (BioTek, Winooski, USA). Each concentration was conducted in three individual experiments and calculated the IC50 to assess the cell proliferation.

Transwell assay

Matrigel (BD Bioscience, Franklin Lakes, USA) was thawed at 4°C, and diluted with a 1 mg/ml final concentration within 100 μl serum free-cold cell culture medium and gel and placed

into the upper chamber of 24-well transwells. The tumor cell population with 1 × 10^6/ml density was sub-cultured on the matrigel. The lower chamber of the transwell was filled with 600 μl culture medium containing 5 μg/ml fibronectin. An adhesive substrate was incubated at 37°C for 24 h. The plates were removed from the transwells and stained with Triarylmethane dye Methanol Diff-Quick solution I (Yeasen, China) for 15 s and washed in solution II for another 15 s. The invaded cells were counted under a light microscope for evaluating cell invasion after air drying.

TUNEL assay

The 6-well plate was fixed by 4% paraformaldehyde for 1 h at room temperature and washed by PBS, then blocked with 3% H_2O_2 methanol solution at room temperature for 10 min, and permeabilized using 0.1% Triton X-100. TUNEL reaction mixture (Roche, USA) was freshly prepared by mixing label solution and enzyme solution (9:1) together and incubated with cells at 37°C for 60 min in a humidified atmosphere in the dark. After 3 times washing with PBS, cells were detected in the 515-565 nm wavelength. Apoptotic index was calculated using the following formula: Apoptotic value = (positive cell number/total cell number) * 100%.

Western blot

Cells with a density of approximately 70-80% were removed from the medium and washed by cold PBS twice, then added 200 μl SDS loading buffer (100 mM Tris-HCl pH = 6.8, 4% SDS, 0.2% bromophenol blue, 20% glycerol, 200 mM DTT), and gently transferred the total proteins into a new eppendorf tube. After performing protein denaturalization at 100°C for 10 min, samples were loaded on 10% SDS-PAGE gel and the proteins were separated under 90 V for 2 h, then transferred onto the nitrocellulose membranes under 30 V at 4°C overnight. 10% non-fat milk was used to block the non-specific antigens at 4°C at least for 6 h. Primary antibodies of TCF4 (1:2000) and β-actin (1:5000) (CST, USA) were added and incubated for 2 h, then followed by the horseradish peroxidase-conjugated secondary antibodies (1:10000) for 1 h at room temperature. Protein bands were detected by ECL Plus (Solarbio, USA) and analyzed using Image J. β-actin was used as a loading control.

Chromatin immunoprecipitation (ChIP)

Cells were fixed in 1% paraformaldehyde and quenched by 0.125 M glycine in room temperature. After washing by PBS, cells were treated with lysis buffer and sonicated (90 cycles of 30 s on/30 s off with high power) into 200-300 bp. 10% whole cell lysis were stored as input. 1 μg antibodies of TCF4 and β-catenin (Abcam, Cambridge, UK) were respectively incubated with the rest of lysis at 4°C overnight, followed by an additional 2 hour-pull down at 4°C by protein-A beads (Thermo Fisher Scientific, Waltham, USA). The beads were washed by 500 mM LiCl and 200 mM NaCl twice, then purified by the DNA phenol-chloroform methods.

qPCR assay

Cells with a density of approximately 70-80% were removed from the medium and washed by cold PBS twice, then added 1 ml RNAiso plus (Takara, Japan) for total RNA extraction and assessed the quality control as well as the concentration using Nanodrop (Thermo Fisher Scientific, USA). 1 μg RNA was conducted reverse transcription using Transcriptor High Fidelity cDNA Synthesis Kit (Roche, USA) and detected the mRNA level using FastStart Universal SYBR Green Master (Roche, USA).

For qPCR, the conditions were set at 95°C for 30 s, followed by 40 cycles of 95°C 5 s, 60°C 10 s, 72°C 30 s. Ct values were harvested to calculate the mRNA levels. Primers designed to encompass about 150 bp around the target regions were listed in **Table 2**.

RNA-seq

Total RNA of A431 cells was extracted using Trizol (Thermo Fisher Scientific, USA) according to the manufacturer's protocol. 2 μg of RNA in each group were used for library preparation by NEBNext Ultra Directional RNA Library Prep Kit for Illumina (NEB, USA) following manufacturer's recommendations and were sequenced on an Illumina Hiseq platform. The raw data was trimmed adaptors and filter out low quality reads using Trimmomatic [8], and checked the quality of clean reads using Fastqc [9]. Next, clean reads were aligned to the latest human genome assembly hg38 using Hisat2 [10]. The transcripts were assembled and the expression

Table 2. All the primers and nucleotides used in this study are listed

Gene symbol	Sequence
TCF4	F: 5'-GCTCCTCCGATTCCGAGG-3'
	R: 5'-TGTTAGAGACAATGTGT-3'
β-actin	F:5'-CTCCCTGGAGAAGAGCTACGAGC-3'
	R: 5'-CCAGGAAGGAAGGCTGGAAGAG-3'
BLOC1S5-TXNDC5	F: 5'-AGGGTCCGATCGATGGGAGC-3'
	F: 5'-TTCGTTATCGTTATGCTAC-3'
ZNF497	F: 5'-ACGGCTGCGGGCGAGCTAGC-3'
	F: 5'-ACCGGGCGTGCTAGCCC-3'
FP565260.2	F: 5'-CGGCTGCCCTTGGCCCGAC-3'
	F: 5'-AGGCATCTAGCTCCAAAAAT-3'
TBC1D3	F: 5'-ACCATGGCTGAAGTGGACC-3'
	F: 5'-TGTTTTTGACCTGGGACCA-3'
UGT1A5	F: 5'-CCACAATTTAGGAAAAACA-3'
	F: 5'-AAGGGGTGCTGGGGTGCA-3'
AD000671.1	F: 5'-AGCTGGGCGATGGGTGCTGA-3'
	F: 5'-GTGTGCGTGGCAAGCCA-3'
AL159163.1	F: 5'-TGTTGGCGTGCAGGCAA-3'
	F: 5'-CCGTGGGGGCTGGAAAGG-3'
ARL2-SNX15	F: 5'-CCGGTAAACCAAATGAAA-3'
	F: 5'-ACAGGTGGGCCAGGAACA-3'
ALDH8A1	F: 5'-TTGGGGTGCATGTTAATTG-3'
	F: 5'-ACTGGTGTGCTGATGCTGA-3'
DRICH1	F: 5'-TGGTGCATGTGCGATGCTGA-3'
	F: 5'-ACCTAGTGAGTCGAGACAA-3'

levels were estimated with FPKM values using the StringTie algorithm with default parameters [11]. Differential mRNA and lncRNA expression among the groups were evaluated using an R package Ballgown [12], and we computed the significance of differences by the Benjamini & Hochberg (BH) *p*-value adjustment method. Gene annotation is described by Ensembl genome browser database (http://www.ensembl.org/index.html). The R package ClusterProfiler was used to annotate the differential genes with gene ontology (GO) terms and Kyoto Encyclopedia of Genes and Genomes (KEGG) pathways [13]. RNA sequencing data was deposited to ArrayExpress assigned with the accession number E-MTAB-7372.

Statistical analysis

The experimental data was processed with SPSS 20 software. Students't-test was used for comparison of the difference between groups. *p*-value less than 0.05 was were considered as statistical significance.

Results

The expression of TCF4 in human cSCC tissues

Initially, ten cases of human cSCC and paired adjacent tissues were investigated with the expression of TCF4. We observed substantially high expression of TCF4 in cSCCs compared to normal control (**Figure 1A**). Meanwhile, the abundant distribution of β-catenin in nucleus suggested that wnt/β-catenin signaling pathway was aberrantly activated in cSCCs (**Figure 1B**). Taken together, our data validated that TCF4 was up-regulated in skin cancers.

Verification of silenced TCF4 in A431 cSCC cells

Next, the effect of TCF4 RNAi was tested in A431 cells using different siRNAs, and processing times. We observed that the transcriptional level of TCF4 was obviously blocked upon siRNA_1 until 48 h compared to the blank (BL) and negative control (NC) groups (**Figure 2A**). TCF4 was slightly elevated at 72 h compared to 48 h, which indicated that the transient transfection of siRNA might gradually lose the efficacy after 48 h. Consistent with the change of mRNA, the decrease of TCF4 protein level was also validated (**Figure 2B**), which indicated that TCF4 silencing A431 cell model was well prepared. The effect of TCF4 silencing was furthermore studied in A431 cells. We observed that TCF4 knockdown could suppress the cell proliferation (**Figure 2C**) and invasion (**Figure 2D**), as well as enhance the cell apoptosis (**Figure 2E**). Collectively, Interference of TCF4 expression played a tumor repressive role in cSCC.

The differential expressed genes upon TCF4 silencing in A431 cells

Next, we harvested A431 cells treated with siRNA_1 in a period of 48 h for transcriptome sequencing. Deep sequencing of mRNA libraries generated a total 192 M, 200 M, and 162 M reads in NC, BL, and TCF4 silencing groups respectively and mapped to the human genome 38 (Ensemble Genomes release 92) using HISAT2. Approximately 80% reads were uniquely mapped and 20% of these reads were mismatches. Furthermore, less than 1.5% of all

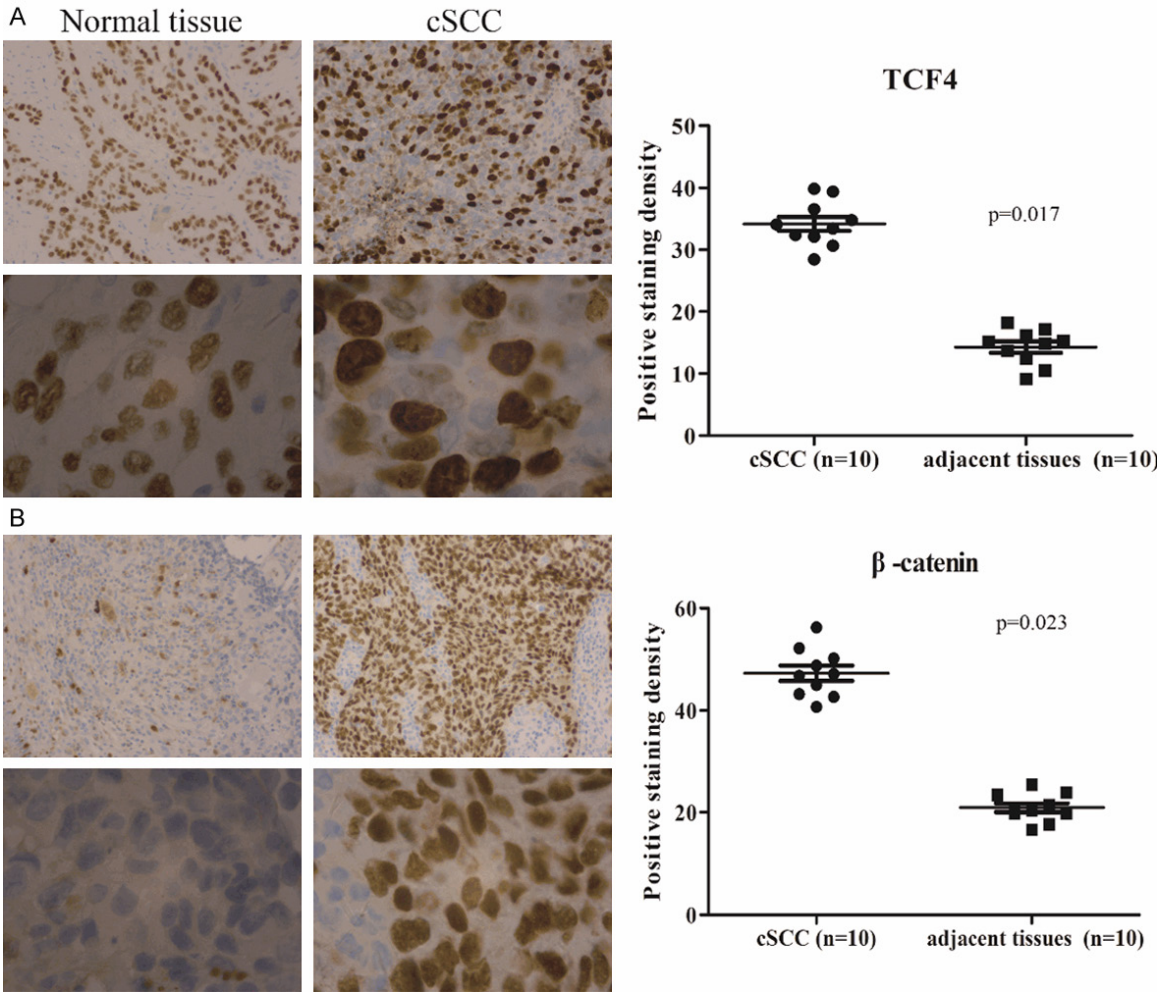

Figure 1. The expression of TCF4 in cSCC tissues. Immunohistochemical analysis of TCF4 (A) and β-catenin (B) in cSCC cancer tissues.TCF4 and β-catenin positive cell nuclei are also detected in the cSCC (20 ×). Magnified images (100 ×) are shown at the bottom. Data is presented as the mean ± standard error of the mean of five picked individual fields.

reads mapping to rRNAs indicated the high quality of our RNA libraries preparation without poly-A selection (**Table 3**). StringTie was used to quantify the gene expression with FPKM distribution (**Figure 3A**) and presented the differentially expressed genes among the three groups. Hierarchical clustering analyzed using edgeR revealed that the overall transcriptome of BL and NC groups were close to each other compared to TCF4 knockdown group, which suggested that TCF4 knockdown might lead to an obvious transcriptional alteration of downstream genes (**Figure 3B**). A total of 409 significantly differential expressed mRNAs were harvested, including 147 up-regulation and 172 down-regulation in A431 cells with TCF4 silencing compared to two controls (**Figure 3C**). The apparent decrease of TCF4 (FC = 0.06684, q = 1.17E-15 vs BL and FC = 0.07793, q = 6.01E-14 vs NC) was confirmed the successful cell model of TCF4 silencing in our study. Furthermore, the top ten differentially up- or down-regulated mRNAs were observed more than ten-fold change in TCF4 silencing groups compared to two control groups (**Table 4**).

The gene ontology analysis of differentially expressed genes in A431 cells induced by TCF4 silencing

Next, the differentially expressed genes were characterized by the functional and signaling pathway enrichment using the GO analysis. The differential mRNAs enrolled in 319 BPs, 19

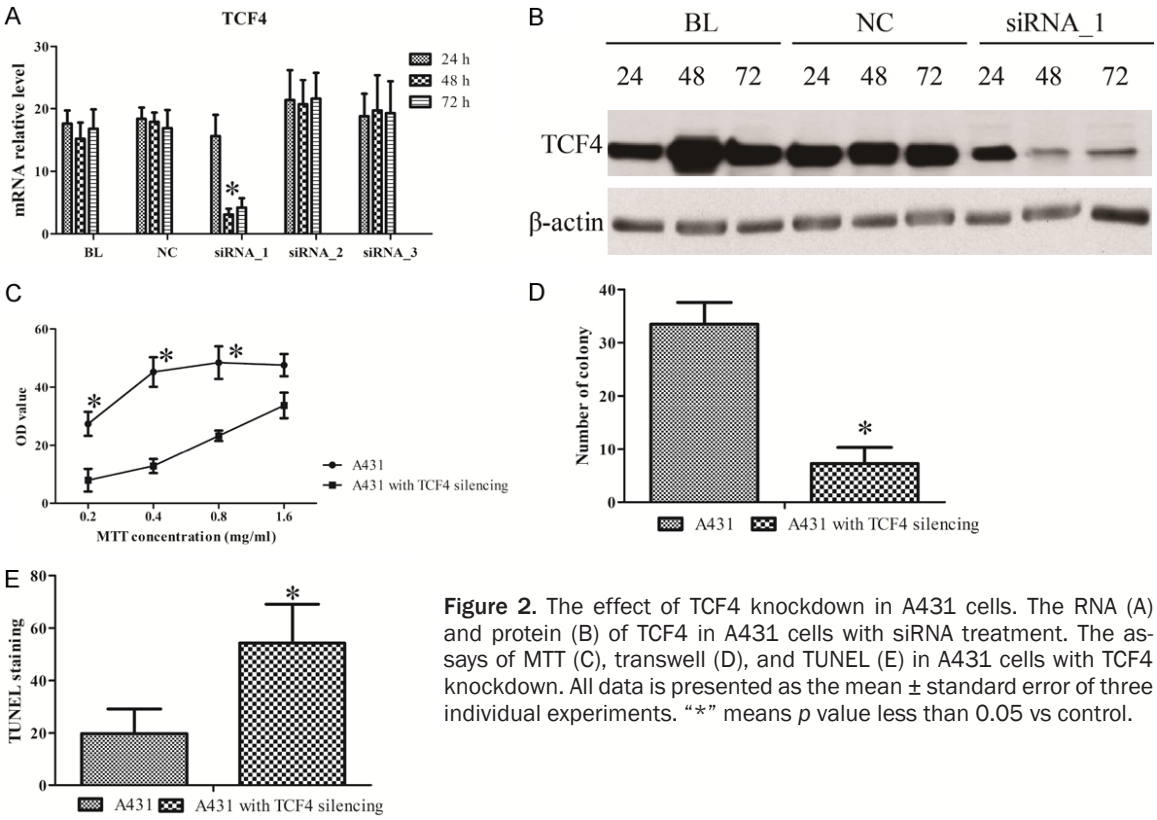

Figure 2. The effect of TCF4 knockdown in A431 cells. The RNA (A) and protein (B) of TCF4 in A431 cells with siRNA treatment. The assays of MTT (C), transwell (D), and TUNEL (E) in A431 cells with TCF4 knockdown. All data is presented as the mean ± standard error of three individual experiments. "*" means *p* value less than 0.05 vs control.

CCs, and 27 MFs were shown the top 20 classifications (**Figure 4A**). Besides Wnt/β-catenin signaling pathway, we also noticed that other GO terms such as cell cycle, reactive oxygen species, and cell proliferation regulation were tightly connected with TCF4 silencing. Furthermore, KEGG pathway enrichment analysis on the differentially expressed mRNAs showed that 22 pathways such as MAPK, Insulin, FoxO, and Rap1 signaling pathways were associated with TCF4 silencing (**Figure 4B**).

The effect of wnt/β-catenin signaling pathway regulated by TCF4 silencing

To explore the mechanism of the transcription change of the differential expressed genes from RNA-seq, ChIP-qPCR of TCF4 and β-catenin were performed to investigate the top ten down-regulated genes. Besides the remarkable down-regulation of TCF4 enrichment (**Figure 5A**), β-catenin was also observed to weaken the binding ability on the promoters of these genes in A431 cells with TCF4 silencing compared to the untreated A431 (**Figure 5B**). However, in untreated A431 cells, we found that ALDH8A1, DRICH1, and UGT1A5 were highly enriched by TCF4 but not β-catenin, which implied that TCF4 might regulate gene expression via wnt/β-catenin dependent and independent ways in cSCC. Collectively, our results showed that TCF4 silencing led to the down-regulation of plenty of genes.

Discussion

TCF4 encodes a high mobility group (HMG) box-containing transcription factor, and is widely expressed in multiple cell types, including brain, fat, endometrium, bladder, lung, ovary, and placenta [14] and functions in many cell lineage specific functions, such as development of lymphocytes, neurogenesis, myogenesis, erythrogenesis, and melanogenesis [15, 16]. Moreover, TCF4 also plays a crucial role in regulating the development of colorectal cancer [17], osteosarcoma [7], hepatocellular carcinoma [18], and glioma [19], which is consistent with our results in cSCC tissues (**Figure 1**). Moreover, our results present that TCF4 knockdown can exert an inhibitory effect on the ability of cSCC growth and invasion (**Figure 2C-E**), which suggests that TCF4 plays a conservative role in various types of cancer.

Table 3. The summary of RNA-seq data

Sample name	TCF4 silencing-1	TCF4 silencing-2	TCF4 silencing-3	BL-1	BL-2	BL-3	NC-1	NC-2	NC-3
Raw reads	59346774	50942620	51720876	66320140	62381800	71570870	75780786	59406874	57284324
Total Raw Bases	8902016100	7641393000	7758131400	9948021000	9357270000	10735630500	11367117900	8911031100	8592648600
Clean reads	57622428	49050358	49702562	64953840	61164470	70274744	74029002	57709138	55874626
Total Clean Bases	8538237820	7206368995	7250768344	9335013886	8737262491	10032724492	10531848522	8454245384	8198181238
Mapped Reads	54826548	46247765	47532757	61942552	58392210	67550514	70744365	54326922	53369303
Mapped Ratio	95.15%	94.29%	95.63%	95.36%	95.47%	96.12%	95.56%	94.14%	95.52%
Uniqed Mapped Reads	45051633	38200608	39142453	51515467	48568769	56467620	59137519	44646460	44184233
Uniqed Mapped Ratio	78.18%	77.88%	78.75%	79.31%	79.41%	80.35%	79.88%	77.36%	79.08%
mismatch Ratio	21.57%	20.94%	20.73%	20.24%	20.45%	19.76%	19.70%	21.00%	20.59%
rRNA Ratio	1.12%	1.13%	0.81%	1.51%	1.51%	1.55%	1.38%	1.32%	1.47%

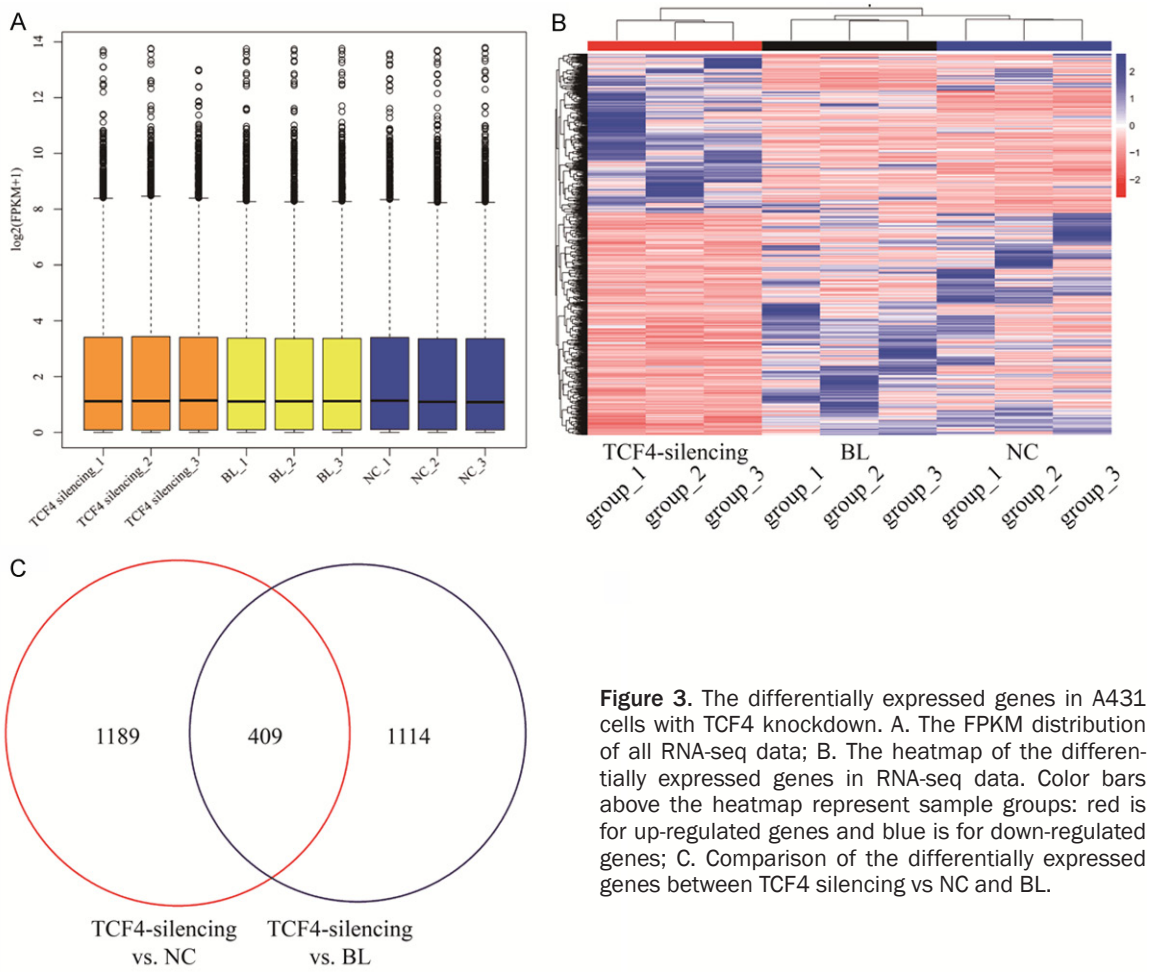

Figure 3. The differentially expressed genes in A431 cells with TCF4 knockdown. A. The FPKM distribution of all RNA-seq data; B. The heatmap of the differentially expressed genes in RNA-seq data. Color bars above the heatmap represent sample groups: red is for up-regulated genes and blue is for down-regulated genes; C. Comparison of the differentially expressed genes between TCF4 silencing vs NC and BL.

TCF family as one of the responders of Wnt/β-catenin signaling pathway in nucleus, can be activated by β-catenin and regulate the transcriptional activity of downstream targets [20]. In the absence of Wnt signaling, repressive TCFs such as TCF3 are bound to Wnt-responsive cis-regulatory modules (W-CRMs). Transducing-like enhancer of split (TLE) family likely play a role in repression of many targets in the absence of activated β-catenin signaling. Upon Wnt stimulation, TCF3 is replaced by activating TCFs such as TCF1, and TCF4, which recruit β-catenin and other co-activators on W-CRMs. Nevertheless, TCFs are also found to function as an additional β-catenin-independent manner in the absence of Wnt signaling [21]. To date, the presence of multiple TCFs in vertebrates supports that different TCFs have specialized transcriptional functions [22]. TCF4 displays a more dedicated and higher binding affinity to TLEs compared to other members. In present study, the cutaneous squamous cell carcinoma of A431 cells showed 359 significantly expressed genes upon TCF4 silencing compared with the negative control. And we observe that TLE2 is obviously up-regulated after TCF4 silencing, which indicates that TLE2 will replace the occupation of TCF4 on W-CRMs after TCF4 direct knockdown even if Wnt/β-catenin signaling is activated. Consistently, GO enrichment and KEGG pathway enrichment analysis both show that Wnt pathway are involved in A431 cells with TCF4 silencing (**Figure 4A**, **4B**). In our case, the intersection of the differentially expressed genes between TCF4 silencing groups vs NC groups and vs BL groups only suggests TLE2 in Wnt/β-catenin signaling pathway, while the union of these two lists of differentially expressed genes includes 58 genes associated with Wnt/β-catenin sig-

Table 4. The top 20 up- and down-regulated coding mRNAs between TCF4 knockdown and BL of A431 cells

Gene_Name	FC (1857/BL)	FC (1857/NC)	Up/down
AC005154.6	30.36893333	30.36893333	UP
AC139530.2	26.10323333	26.10323333	UP
Z84492.1	14.19316667	14.19316667	UP
AC027796.3	8.357439554	13.50260132	UP
MIA	13.16666667	13.16666667	UP
AC034102.2	12.42423333	12.42423333	UP
MMP10	2.359888173	11.40592424	UP
KRT1	2.462159313	11.01678283	UP
TRIM6-TRIM34	9.979466667	9.979466667	UP
URGCP-MRPS24	17.84827142	9.533017713	UP
PCDHGA2	5.878841626	8.183169531	UP
AL121753.1	6.519502008	8.146131155	UP
NTS	3.971182187	7.859366667	UP
PMFBP1	7.8194	7.8194	UP
ABI3BP	2.652916394	7.696448981	UP
KRTDAP	9.097996361	7.651036685	UP
CHRNA3	7.627933333	7.627933333	UP
UGT2A1	3.794288161	7.090133333	UP
MMP12	3.276427312	6.521653282	UP
PCDHGC4	10.4486595	6.469675949	UP
AC007192.1	0.167244252	0.166266976	DOWN
CCK	0.32248702	0.155695335	DOWN
GKN1	0.17356792	0.155074824	DOWN
RBAK-RBAKDN	0.18842055	0.151754505	DOWN
C9orf153	0.233265316	0.150907753	DOWN
ISLR2	0.143325339	0.144711518	DOWN
CLDN24	0.171342411	0.144078379	DOWN
SPRR3	0.202340639	0.142937614	DOWN
AC011499.1	0.104644835	0.125296535	DOWN
DRICH1	0.105618555	0.09633138	DOWN
ALDH8A1	0.402452276	0.095431078	DOWN
ARL2-SNX15	0.012196332	0.094747514	DOWN
TCF4	0.066840154	0.077930377	DOWN
AL159163.1	0.031868853	0.057750725	DOWN
AD000671.1	0.030956334	0.041680734	DOWN
UGT1A5	0.02104863	0.030842057	DOWN
TBC1D3	0.037179374	0.025986581	DOWN
FP565260.2	0.003968639	0.015417036	DOWN
ZNF497	0.021368889	0.015368627	DOWN
BLOC1S5-TXNDC5	0.000409573	0.001191535	DOWN

naling pathway, such as TCF7, WNT2B, WNT3A, WNT7B, and WNT8B. Given the results above, we declare that TCF4 silencing substantially impacts Wnt/β-catenin signaling pathway in cutaneous squamous cell carcinoma cells.

Among differentially expressed mRNAs, PIK3R3 [23], SPRR3 [24], SSTR5 [25], UCP3 [26], and TREM1 [27] were previously identified in other skin related diseases. Beyond that, we also notice that MAPK, Insulin, and Rap1 signaling pathways are impacted by TCF4 knockdown in A431 cells. These pathways were previously determined to connect with TCF4 in other diseases or tissues, which is consistent with previous studies. For example, MAPK pathway could antagonize the activity of Wnt/β-catenin and change the abundance of TCF4 in intestine [28, 29], while Insulin and Rap1 signaling can both affect β-catenin then regulate the down-stream targets in breast cancer and squamous cell carcinoma [30, 31].

Finally, when we were validating the transcriptional regulation of the differentially expressed genes controlled by TCF4, we unexpectedly noticed that ALDH8A1, DRICH1, and UGT1A5 are highly enriched by TCF4, but not β-catenin in untreated A431 cells (**Figure 5B**), which implies that in cSCC cells with TCF4 aberrant activation, TCF4 may play a wnt/β-catenin independent role in gene transcription regulation. Given this observation, only inhibition of Wnt/β-catenin may not be enough to govern the entire transcriptome affected by TCF4 derived gene regulation.

In summary, our findings declared that TCF4 played an important role in tumorigenesis of skin cancer via the aberrant activation of variety of signaling pathways, and could be considered as a potential therapeutic target for cSCC treatment.

Acknowledgements

This work was funded by the National Natural Science Foundation of China (No. 81573070).

Disclosure of conflict of interest

None.

Address correspondence to: Dr. Xichuan Yang, Department of Dermatology, The First Affiliated Hospital of The Army Medical University, 29 Gaotanyan

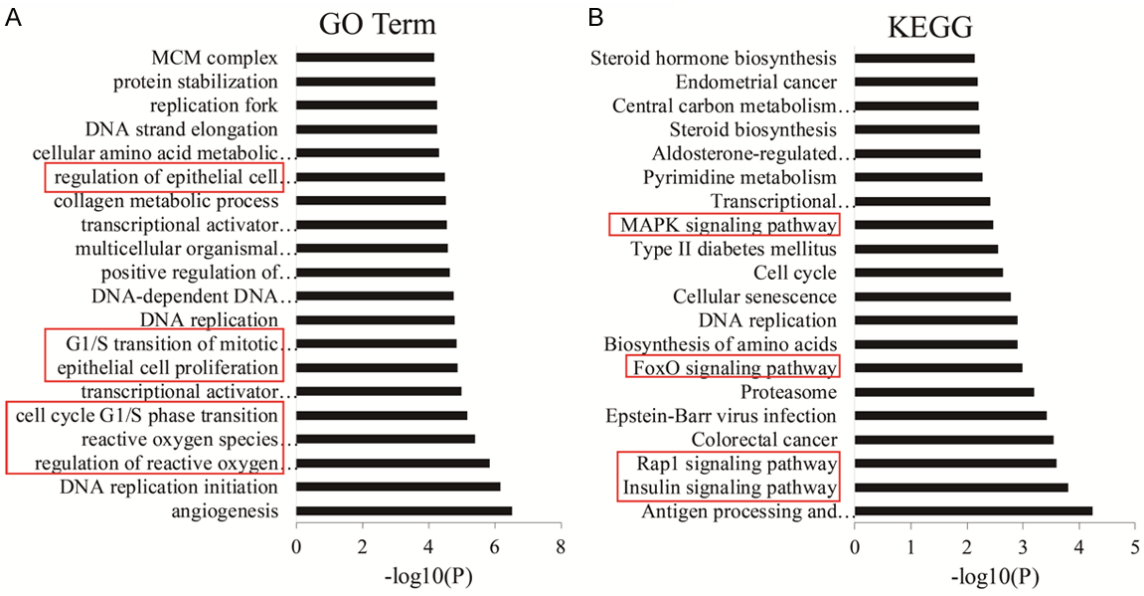

Figure 4. Functional classification and pathway analysis of differentially expressed genes. (A) Gene ontology (GO) and (B) KEGG analysis of differentially expressed genes of TCF4 silencing vs NC and BL.

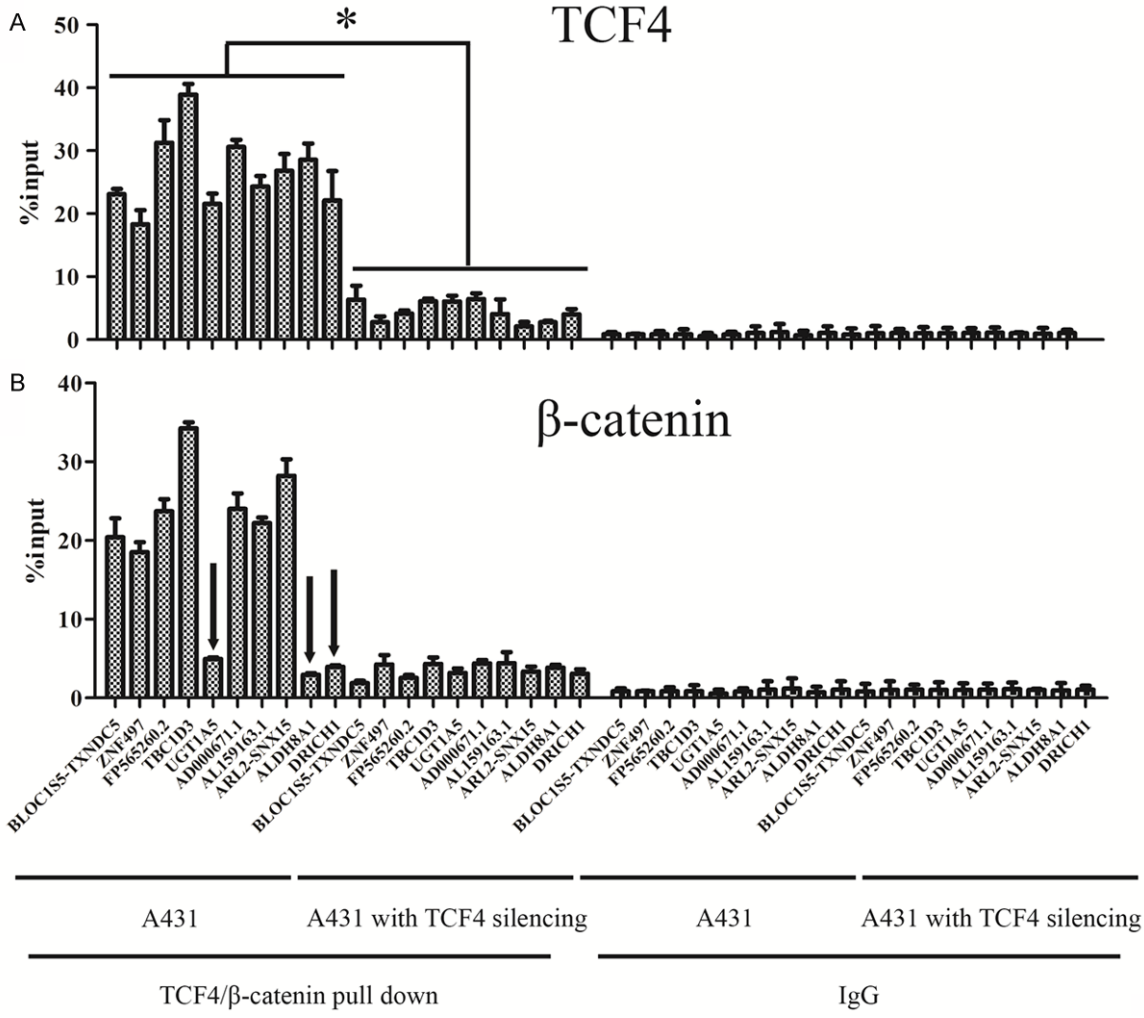

Figure 5. The enrichment of TCF4 and β-catenin on the differential expressed genes. ChIP assay analysis of TCF4 (A) and β-catenin (B) in A431 cells with TCF4 silencing. "*" means *p* value less than 0.05 vs control. ALDH8A1, DRICH1, and UGT1A5 were highlighted by black arrow heads.

Street, Shapingba District, Chongqing 400038, P.R. China. E-mail: doctoryxc@msn.com

References

[1] Kivisaari A and Kahari VM. Squamous cell carcinoma of the skin: emerging need for novel biomarkers. World J Clin Oncol 2013; 4: 85-90.

[2] Zhang L, Qin H, Wu Z, Chen W and Zhang G. Pathogenic genes related to the progression of actinic keratoses to cutaneous squamous cell carcinoma. Int J Dermatol 2018; 57: 1208-1217.

[3] Kabir S, Schmults CD and Ruiz ES. A review of cutaneous squamous cell carcinoma epidemiology, diagnosis, and management. 2018.

[4] Hufbauer M, Cooke J, van der Horst GT, Pfister H, Storey A and Akgul B. Human papillomavirus mediated inhibition of DNA damage sensing and repair drives skin carcinogenesis. Mol Cancer 2015; 14: 183.

[5] Davidsen J, Larsen S, Coskun M, Gogenur I, Dahlgaard K, Bennett EP and Troelsen JT. The VTI1A-TCF4 colon cancer fusion protein is a dominant negative regulator of Wnt signaling and is transcriptionally regulated by intestinal homeodomain factor CDX2. PLoS One 2018; 13: e0200215.

[6] Duan J, He Y, Fu X, Deng Y, Zheng M and Lu D. CDK7 activated beta-catenin/TCF signaling in hepatocellular carcinoma. Exp Cell Res 2018; 370: 461-467.

[7] Li R, Liu S, Li Y, Tang Q, Xie Y and Zhai R. Long noncoding RNA AFAP1AS1 enhances cell proliferation and invasion in osteosarcoma through regulating miR46955p/TCF4betacatenin signaling. Mol Med Rep 2018; 18: 1616-1622.

[8] Bolger AM, Lohse M and Usadel B. Trimmomatic: a flexible trimmer for Illumina sequence data. Bioinformatics 2014; 30: 2114-2120.

[9] Andrews S. FastQC a quality control tool for high throughput sequence data. 2013.

[10] Kim D, Langmead B and Salzberg SL. HISAT: a fast spliced aligner with low memory requirements. Nat Methods 2015; 12: 357-360.

[11] Pertea M, Pertea GM, Antonescu CM, Chang TC, Mendell JT and Salzberg SL. StringTie enables improved reconstruction of a transcriptome from RNA-seq reads. Nat Biotechnol 2015; 33: 290-295.

[12] Frazee AC, Pertea G, Jaffe AE, Langmead B, Salzberg SL and Leek JT. Ballgown bridges the gap between transcriptome assembly and expression analysis. Nat Biotechnol 2015; 33: 243-246.

[13] Yu G, Wang LG, Han Y and He QY. clusterProfiler: an R package for comparing biological themes among gene clusters. OMICS 2012; 16: 284-287.

[14] Fagerberg L, Hallstrom BM, Oksvold P, Kampf C, Djureinovic D, Odeberg J, Habuka M, Tahmasebpoor S, Danielsson A, Edlund K, Asplund A, Sjostedt E, Lundberg E, Szigyarto CA, Skogs M, Takanen JO, Berling H, Tegel H, Mulder J, Nilsson P, Schwenk JM, Lindskog C, Danielsson F, Mardinoglu A, Sivertsson A, von Feilitzen K, Forsberg M, Zwahlen M, Olsson I, Navani S, Huss M, Nielsen J, Ponten F and Uhlen M. Analysis of the human tissue-specific expression by genome-wide integration of transcriptomics and antibody-based proteomics. Mol Cell Proteomics 2014; 13: 397-406.

[15] Sepp M, Kannike K, Eesmaa A, Urb M and Timmusk T. Functional diversity of human basic helix-loop-helix transcription factor TCF4 isoforms generated by alternative 5' exon usage and splicing. PLoS One 2011; 6: e22138.

[16] In 't Hout FEM, van Duren J, Monteferrario D, Brinkhuis E, Mariani N, Westers TM, Chitu D, Nikoloski G, van de Loosdrecht AA, van der Reijden BA, Jansen JH, and Huls G. TCF4 promotes erythroid development. Exp Hematol 2019; 69: 17-21, e1.

[17] Li T, Jian X, He H, Lai Q, Li X, Deng D, Liu T, Zhu J, Jiao H, Ye Y, Wang S, Yang M, Zheng L, Zhou W and Ding Y. MiR-452 promotes an aggressive colorectal cancer phenotype by regulating a Wnt/beta-catenin positive feedback loop. J Exp Clin Cancer Res 2018; 37: 238.

[18] Wu N, Zhao J, Yuan Y, Lu C, Zhu W and Jiang Q. NOP7 interacts with beta-catenin and activates beta-catenin/TCF signaling in hepatocellular carcinoma cells. Onco Targets Ther 2018; 11: 6369-6376.

[19] Liu Z, Song J, Wu Y, Yao S, Xu GZ and Diao B. Expression and functional analysis of TCF4 isoforms in human glioma cells. Mol Med Rep 2018; 17: 6023-6027.

[20] Daniels DL and Weis WI. Beta-catenin directly displaces Groucho/TLE repressors from Tcf/Lef in Wnt-mediated transcription activation. Nat Struct Mol Biol 2005; 12: 364-371.

[21] Hrckulak D, Janeckova L, Lanikova L, Kriz V, Horazna M, Babosova O, Vojtechova M, Galuskova K, Sloncova E and Korinek V. Wnt effector TCF4 is dispensable for Wnt signaling in human cancer cells. Genes (Basel) 2018; 9.

[22] Ramakrishnan AB, Sinha A, Fan VB and Cadigan KM. The Wnt transcriptional switch: TLE removal or inactivation? Bioessays 2018; 40.
[23] Ji ZH, Chen J, Gao W, Zhang JY, Quan FS, Hu JP, Yuan B and Ren WZ. Cutaneous transcriptome analysis in NIH hairless mice. PLoS One 2017; 12: e0182463.
[24] Trzeciak M, Sakowicz-Burkiewicz M, Wesserling M, Dobaczewska D, Glen J, Nowicki R and Pawelczyk T. Expression of cornified envelope proteins in skin and its relationship with atopic dermatitis phenotype. Acta Derm Venereol 2017; 97: 36-41.
[25] Hagstromer L, Emtestam L, Stridsberg M and Talme T. Expression pattern of somatostatin receptor subtypes 1-5 in human skin: an immunohistochemical study of healthy subjects and patients with psoriasis or atopic dermatitis. Exp Dermatol 2006; 15: 950-957.
[26] Lago CU, Nowinski SM, Rundhaug JE, Pfeiffer ME, Kiguchi K, Hirasaka K, Yang X, Abramson EM, Bratton SB, Rho O, Colavitti R, Kenaston MA, Nikawa T, Trempus C, Digiovanni J, Fischer SM and Mills EM. Mitochondrial respiratory uncoupling promotes keratinocyte differentiation and blocks skin carcinogenesis. Oncogene 2012; 31: 4725-4731.
[27] Hyder LA, Gonzalez J, Harden JL, Johnson-Huang LM, Zaba LC, Pierson KC, Eungdamrong NJ, Lentini T, Gulati N, Fuentes-Duculan J, Suarez-Farinas M and Lowes MA. TREM-1 as a potential therapeutic target in psoriasis. J Invest Dermatol 2013; 133: 1742-1751.
[28] Heuberger J, Kosel F, Qi J, Grossmann KS, Rajewsky K and Birchmeier W. Shp2/MAPK signaling controls goblet/paneth cell fate decisions in the intestine. Proc Natl Acad Sci U S A 2014; 111: 3472-3477.
[29] Ishitani T, Ninomiya-Tsuji J, Nagai S, Nishita M, Meneghini M, Barker N, Waterman M, Bowerman B, Clevers H, Shibuya H and Matsumoto K. The TAK1-NLK-MAPK-related pathway antagonizes signalling between beta-catenin and transcription factor TCF. Nature 1999; 399: 798-802.
[30] Geng Y, Ju Y, Ren F, Qiu Y, Tomita Y, Tomoeda M, Kishida M, Wang Y, Jin L, Su F, Wei C, Jia B, Li Y and Chang Z. Insulin receptor substrate 1/2 (IRS1/2) regulates Wnt/beta-catenin signaling through blocking autophagic degradation of dishevelled2. J Biol Chem 2014; 289: 11230-11241.
[31] Goto M, Mitra RS, Liu M, Lee J, Henson BS, Carey T, Bradford C, Prince M, Wang CY, Fearon ER and D'Silva NJ. Rap1 stabilizes beta-catenin and enhances beta-catenin-dependent transcription and invasion in squamous cell carcinoma of the head and neck. Clin Cancer Res 2010; 16: 65-76.